2011 American Control Conference
on O'Farrell Street, San Francisco, CA, USA
June 29 - July 01, 2011

Stability Derivatives for a Flapping Wing MAV in a Hover Condition Using Local Averaging

Christopher T. Orlowski
Department of Aerospace Engineering
University of Michigan
Ann Arbor, Michigan 48109
Email: cptorlo@umich.edu

Anouck R. Girard
Department of Aerospace Engineering
University of Michigan
Ann Arbor, Michigan 48109
Email: anouck@umich.edu

Abstract— **We present an analytically tractable method of obtaining the stability derivatives for a flapping wing MAV, in the vicinity of a hover condition, using local averaging techniques. The analytical stability derivatives are obtained for the longitudinal equations of motion, under the constraint of symmetrical flapping with respect to the longitudinal axis of the central body. The analysis results in an eigenvalue structure consisting of two stable subsidence modes and one unstable oscillatory mode. Analysis shows a modal structure consistent with the standard VTOL structure. The unstable oscillatory mode is close to the imaginary axis, consistent with the modal structure of hovering helicopters. Scaling properties are consistent with previous numerical results. The method does not require numerically intensive calculations or frequency response analysis to gain an approximation of the stability of a potential flapping wing MAV in the vicinity of a hover condition.**

I. Introduction

Taylor and Thomas in [1] produced a seminal work on the flight stability of a desert locust. Using the small perturbation form of the standard aircraft equations, available in [2], in the vicinity of a hover condition and using experimentally obtained aerodynamic data, Taylor and Thomas obtained the stability derivatives of the desert locust in forward flight. Sun and Xiong in [3] expanded on the work in [1] and conducted the stability analysis of a bumblebee in hover. The stability derivatives are obtained by coupling the standard aircraft equations of motion with the Navier-Stokes Equations. The work is expanded to four additional insect species in [4]. Faruque and Humbert obtained the longitudinal and lateral stability derivatives for a model insect, based off a fruit fly, using System ID techniques in [5] and [6]. Faruque and Humbert obtained the derivatives for both 'haltere on' and 'haltere off' configurations. All of the works result in a similar conclusion that the linearized dynamics of an insect in a hover condition have three main modes: two stable subsidence modes (one fast and one slow) and one unstable, oscillatory mode. The eigenvalues show the same modal structure of many VTOL and rotary wing aircraft, according to the stability derivatives available in [7].

For this analysis, the flapping wing micro-air vehicle (FWMAV) is modeled as a single body. The mass and inertial effects of the wings on the position and orientation of the body are neglected. We only consider the longitudinal motion of the flapping wing under the constraint of symmetrical flapping of the wings, with respect to the longitudinal axis of the body. Through the use of local averaging of the perturbed aerodynamic equations, we obtain the system matrix for a model FWMAV in the vicinity of a hover condition. The perturbations enter through the velocity of the center of pressure of the wing and the effective angle of attack of the wing. The aerodynamic model is a quasi-steady/blade element model. The equilibrium solution for the hover condition is obtained using local averaging, as used in [5], to calculate the average aerodynamic forces and moments. The analysis results in a modal structure consistent with previous analyses: two subsidence modes, one fast and one slow, and one unstable oscillatory mode. The modal structure does not change as the stroke plane angle of the the wings is varied. The modal structure is the most common VTOL aircraft configuration [7] and is independently obtained in [3] and [5]. The small magnitude of the unstable oscillatory mode is consistent with the eigenvalues for rotary wing aircraft in the vicinity of a hover condition and the numerical results presented in [3].

The paper is organized in the following manner. Section II outlines the flapping wing MAV model to be used throughout the analysis. Section III details the equilibrium hover solution for the averaged system. Section IV will detail the calculation of the stability derivatives using local averaging techniques. Section IV-B details the stability derivatives due to changes in the velocity of the wing's center of pressure. Section IV-C details the addition to the stability derivatives from the change in angle of attack of the wing relative to the stroke plane. Section V will present the resulting eigenvalues from the stability derivatives calculations. Section VI will present the Conclusion and Future Work.

II. Flapping Wing MAV Model

The model is based off of work previously conducted on multiple body models of FWMAVs, available in [8]. For reference to the inertial frame, a fixed frame is originated at the center of mass of the central body. The frame, denoted by the B frame, is oriented in accordance with the standard alignment for aircraft. The x-axis points through the nose of the aircraft, y-axis is perpendicular to the x-axis and is positive to the right of the FWMAV. We assume a $x-z$ plane of mass symmetry for the central body and the z-axis is positive downward in the $x-z$ plane. The B frame is

978-1-4577-0079-8/11/$26.00 ©2011 AACC

depicted in Fig. 1.

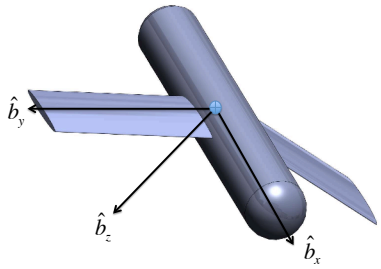

Fig. 1. FWMAV Model with B Frame

The wings in previous work are assumed to have three degrees of freedom relative to the stroke plane at the wing joint. The three degrees of freedom are the deviation angle (δ), the angle of attack (α), and the flapping angle (ζ). In the vicinity of a hover condition, we are going to neglect the deviation angle of the wings. Therefore, the effects of the wings on the central body will be determined by the angle of attack, the flapping angle, and the stroke plane angle β. The angle of attack, α, and the stroke plane angle are depicted in Fig. 2 for the right wing. Fig. 3 shows the flapping angle for the right and left wings.

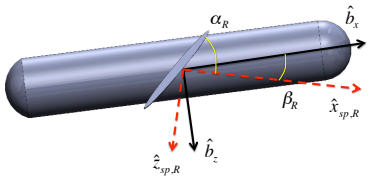

Fig. 2. Stroke Plane Angle, β, and Angle of Attack, α

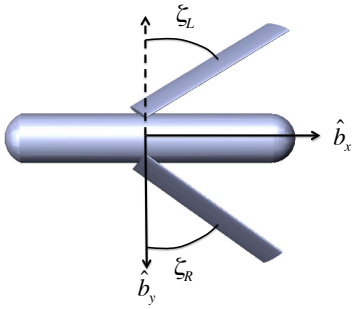

Fig. 3. Flapping Angle ζ

A. Equations of Motion

For an initial analysis, we neglect the mass of the wings and their associated inertial effects on the position and orientation of the central body. We assume that the given aerodynamic model will produce identical normal and tangential forces for symmetrical flapping relative to the central body. Additionally, under the constraint of symmetrical flapping and with the aerodynamic forces assumption, the lateral forces, roll moments, and yaw moments will be identically zero when resolved in the body frame. For longitudinal motion, the equations of motion are

$$\dot{u} = \frac{F_x}{m_{sys}} - g\sin\theta - q\,w, \tag{1}$$

$$\dot{w} = \frac{F_z}{m_{sys}} + g\cos\theta + q\,u, \tag{2}$$

$$\dot{\theta} = q, \tag{3}$$

and

$$\dot{q} = \frac{M}{I_{yy}}. \tag{4}$$

The mass of the system is denoted by m_{sys} and the moment of inertia with respect to $\hat{b}_y$ of the B frame is I_{yy}. The wings are assumed to be mounted at joints such that their y-position in the B frame are equal in magnitude, but opposite in sign. The x- and z-positions of the wings joints in the B frame are identically zero.

B. Aerodynamic Model

The aerodynamic model is based off of the model used extensively in [9] and [10]. We will make a simplifying assumption that the angle of attack is constant during each half-stroke, therefore the normal force contribution due to rotation of the wing will be zero. The assumption was previously used in [11], [12], [13], and [14]. The wing is assumed to flip instantly at the end of each half-stroke. As a result, we can write the angle of attack as a function of time as

$$\alpha(t) = \text{sign}(\dot{\zeta})\alpha_m, \tag{5}$$

where $\dot{\zeta}$ denotes the time rate of change of the flapping angle of the wing. The flapping angle will be a sinusoidal function, defined by:

$$\zeta(t) = \zeta_m \sin(2\pi f t), \tag{6}$$

where ζ_m is half of the total flapping amplitude. The tangential and normal forces on the wing are calculated according to

$$F_T = \frac{1}{2}\rho A_w C_T U_{cp}(t)^2 \text{ and } F_N = \frac{1}{2}\rho A_w C_N U_{cp}(t)^2. \tag{7}$$

The coefficients for the tangential and normal tangential forces are calculated according to

$$C_T = -0.4\,\text{sign}\left(\dot{\zeta}\right)\cos^2(2\alpha_m) \tag{8}$$

and

$$C_N = -3.4\sin(\alpha_m). \tag{9}$$

The coefficients are modified from [9] consistent with the choice of wing kinematics. In Eqs. (8) and (9), α_m is the constant amplitude of the angle of attack during the upstroke and the downstroke. If the translational and angular velocity of the body is neglected in the calculation of aerodynamic forces and moments, then the velocity at the center of pressure of the wing is

$$U_{cp}(t) = \hat{r}_2 b\,(\omega\zeta_m)\cos(\omega t). \tag{10}$$

The normal and tangential forces generated by the motion of the wing are transformed into the body frame. The transformation is obtained through a series of rotations from the wing frame to the stroke plane frame and from the stroke plane frame to the body frame. The wings are assumed to be thin, rigid flat plates with constant chord, c, and semi-span, b. The center of pressure of the wing is calculated to be at the normalized center of pressure, $\hat{r}_2$, and $^1/_4$ of the chord from the leading edge of the wing, based on the chosen wing geometry.

III. Hover Solution

The hover solution is obtained through the use of local averaging. A treatment of local averaging is available in [15]. The aerodynamic forces and moments are averaged over one flapping cycle, according to

$$\overline{y} = \frac{1}{2\pi}\int_0^{2\pi} y(t)dt\,, \tag{11}$$

where $y(t)$ is representative of the aerodynamic force or moment equation. Based on the chosen aerodynamic model and representation of the flight dynamics, the averaged thrust force in the stroke plane frame is zero, identical to the result obtained in [11]. The averaged thrust force in the stroke plane frame, for one wing, is equal to

$$\overline{F}_{z,sp} = -\frac{17}{40}\rho\, A_w \sin\left(2\alpha_m\right)\left(\hat{r}_2 b\,\omega\zeta_m\right)^2. \tag{12}$$

In (12), A_w is the area of the wing and ω is equal to $2\pi f$. The average of the aerodynamic pitching moment is zero, identical to the result in [11], due to the assumptions on wing joint placement. Therefore, a hover solution in the B frame is obtained when the averaged thrust is zero and the averaged lift is equal to weight. If the stroke plane is inclined relative to the longitudinal axis of the body, then the following two conditions will need to be met:

$$\overline{F}_z\cos\beta = m_{sys}g\cos\theta_o \text{ and } \overline{F}_z\sin\beta = m_{sys}g\sin\theta_o, \tag{13}$$

where θ_o denotes the nominal pitch attitude.

IV. Stability Derivatives

A. Perturbed Aerodynamics

The stability derivatives are obtained using a combination of averaging and a perturbed aerodynamic model. First, the perturbed velocity of the body needs to be written in the respective wing frames according to

$$\Delta\bar{\mathbf{v}}_b^w = \mathbf{R}_\zeta\mathbf{R}_\beta\begin{bmatrix}\Delta u\\ \Delta w\end{bmatrix}, \tag{14}$$

where $\mathbf{R}_\beta$ denotes the rotation matrix carrying the body frame to the stroke plane frame. The matrix $\mathbf{R}_\zeta$ details the rotation matrix carrying the stroke plane angle to the wing frame when the flapping angle is non-zero. In component form, the perturbed translational velocity of the body in the wing frame is:

$$\Delta\bar{\mathbf{v}}_b^w = \begin{bmatrix}\cos\zeta\left(\cos\beta\Delta u - \sin\beta\Delta w\right)\\ \sin\beta\Delta u + \cos\beta\Delta w\end{bmatrix}. \tag{15}$$

The pitch velocity of the body is transformed into the wing frame according to

$$\Delta\bar{\omega}_b^w = \mathbf{R}_\zeta\mathbf{R}_\beta\begin{bmatrix}0 & \Delta q & 0\end{bmatrix}^{\mathrm{T}}. \tag{16}$$

The resulting total velocity of the wing, in the wing frame, is

$$\bar{\mathbf{v}}_{wing} = \begin{bmatrix}\hat{r}_2 b\,\dot{\zeta}\\ 0\end{bmatrix} + \Delta\bar{\mathbf{v}}_b^w + \Delta\bar{\omega}_b^w\times\bar{\rho}_{ac}^w. \tag{17}$$

The aerodynamic center of pressure in the wing frame, relative to the body frame, is expressed as $\bar{\rho}_{ac}^w$. The magnitude of the wing velocity squared, neglecting Δ^2 terms, is

$$||\bar{\mathbf{v}}_{wing}||^2 = (\hat{r}_2 b\dot{\zeta})^2 + (\Delta\bar{\mathbf{v}}_b^w\cdot\hat{b}_x + \Delta\bar{\omega}_b^w\cdot\hat{b}_x)\hat{r}_2 b\dot{\zeta}. \tag{18}$$

The first term, $(\hat{r}_2 b\dot{\zeta})^2$, accounts for the averaged lift/thrust force in the hover solution. Therefore, the perturbations to the aerodynamic forces and moments will result from the second and third terms. The hover solution is subtracted from the perturbed aerodynamics equations obtained from the equations of motion in vicinity of a hover condition; a more detailed treatment is available in [2] and [5]. Therefore, with the velocity perturbations accounted for in the aerodynamic force and moment calculations and after eliminating the contributions enabling the hover condition, the perturbed equations of motion can be written as:

$$\Delta\dot{u} = X_u(t)\Delta u + X_w(t)\Delta w + X_q(t)\Delta q - g\cos\theta_o\Delta\theta, \tag{19}$$

$$\Delta\dot{w} = Z_u(t)\Delta u + Z_w(t)\Delta w + Z_q(t)\Delta q - g\sin\theta_o\Delta\theta, \tag{20}$$

and

$$\Delta\dot{q} = M_u(t)\Delta_u + M_w(t)\Delta w + M_q(t)\Delta q, \tag{21}$$

where $X_{[.]}$, $Z_{[.]}$, and $M_{[.]}$ are nonlinear functions of the flapping angle and angle of attack. The aerodynamic perturbations do not directly affect the pitch angle of the FWMAV.

B. Velocity Stability Derivatives

In [7], the perturbed hover equations for VTOL aircraft and helicopters neglect a perturbation velocity in the x-direction due to velocity in the z-direction (w). In [5], perturbations are only considered in the longitudinal direction. In this analysis, perturbations to both the longitudinal velocity, Δu, and vertical velocity, Δw, are considered. For brevity in the following equations, we define the following coefficients:

$$c_T = 0.2\rho\, A_w\hat{r}_2 b\,\omega\,\zeta_m\cos^2\left(2\alpha_m\right) \tag{22}$$

and

$$c_N = 1.7\rho\, A_w\hat{r}_2 b\,\omega\,\zeta_m\sin\left(\alpha_m\right), \tag{23}$$

which account for the effects of the tangential and normal forces generated on the wings due to motion of the central body. The stability derivatives are arranged in the following manner:

$$\begin{bmatrix}\Delta\dot{u}\\ \Delta\dot{w}\\ \Delta\dot{\theta}\\ \Delta\dot{q}\end{bmatrix} = \bar{\mathbf{A}}_{hover}\begin{bmatrix}\Delta u\\ \Delta w\\ \Delta\theta\\ \Delta q\end{bmatrix}, \tag{24}$$

where the system matrix is arranged according to

$$\bar{\mathbf{A}}_{hover} = \begin{bmatrix} \overline{X}_u & \overline{X}_w & -g\,\cos(\overline{\theta}_o) & \overline{X}_q \\ \overline{Z}_u & \overline{Z}_w & -g\,\sin(\overline{\theta}_o) & \overline{Z}_q \\ 0 & 0 & 0 & 1 \\ \overline{M}_u & \overline{M}_w & 0 & \overline{M}_q \end{bmatrix}. \quad (25)$$

The overbar denotes average with respect to time t. The mass and moment of inertia about the y-axis of the central body are absorbed into the stability derivatives in $\bar{\mathbf{A}}_{hover}$, such that

$$\overline{X}_u = \frac{2}{m_{sys}} \left(\frac{1}{2\pi} \int_0^{2\pi} X_u(t) dt \right). \quad (26)$$

For example, the nonlinear function describing the effect of longitudinal velocity on the vertical dynamics of the central body, due to the tangential force on the wing is

$$\begin{aligned} Z_{u,T}(t) \quad = \quad & \left(\frac{1}{2} \mathrm{s}(2\beta) \mathrm{c}\alpha_m \mathrm{c}^2\zeta + \mathrm{c}^2\beta \mathrm{s}\alpha_m \mathrm{sign}\left(\dot{\zeta}\right) \mathrm{c}\zeta \right) \ldots \\ & * \mathrm{sign}\left(\dot{\zeta}\right) c_T \cos(\omega t)\, \Delta u, \end{aligned} \quad (27)$$

where 'c' is shorthand for cosine and 's' is shorthand for sine. The averaged result is

$$\overline{Z}_{u,T} = \frac{1}{\pi} \sin(2\beta) \cos(\alpha_m)\, c_T \left(1 + \frac{\sin(2\zeta_m)}{2\zeta_m} \right) \Delta u. \quad (28)$$

The integrals are calculated using assistance from [16] and [17]. The non-zero stability derivatives for the longitudinal motion of the body are

$$\overline{X}_u = -\frac{2}{\pi} \mathrm{c}^2(\beta) \left(\mathrm{c}\alpha_m c_T + \mathrm{s}\alpha_m c_N \right) \left(1 + \frac{\sin(2\zeta_m)}{2\zeta_m} \right) \quad (29)$$

and

$$\overline{X}_w = \frac{1}{\pi} \mathrm{s}(2\beta) \left(\mathrm{c}\alpha_m c_T + \mathrm{s}\alpha_m c_N \right) \left(1 + \frac{\sin(2\zeta_m)}{2\zeta_m} \right). \quad (30)$$

The non-zero stability derivatives for the vertical motion of the body are

$$\overline{Z}_u = \frac{1}{\pi} \mathrm{s}(2\beta) \left(\mathrm{c}\alpha_m c_T + \mathrm{s}\alpha_m c_N \right) \left(1 + \frac{\sin(2\zeta_m)}{2\zeta_m} \right) \quad (31)$$

and

$$\overline{Z}_w = -\frac{2}{\pi} \mathrm{s}^2(\beta) \left(\mathrm{c}\alpha_m c_T + \mathrm{s}\alpha_m c_N \right) \left(1 + \frac{\sin(2\zeta_m)}{2\zeta_m} \right). \quad (32)$$

The results predict that if the stroke plane is zero, namely the main flapping motion is along the longitudinal axis of the central body, then there will be no effect on the motion of the body in the longitudinal direction to a perturbation in the vertical direction. Additionally, the affects on the vertical direction of the body are zero for perturbations in velocity in the vertical and horizontal directions. In [7], Franklin states that the X_w derivative is traditionally neglected.

The stability derivatives in the longitudinal and vertical directions, due to the pitch rate q, are both identically zero. For completeness,

$$\overline{X}_q \equiv 0 \text{ and } \overline{Z}_q \equiv 0, \quad (33)$$

both of which are traditionally neglected due to low magnitude in comparison with the other stability derivatives [7]. The stability derivatives resulting from change in the aerodynamic pitching moment due to perturbations in the longitudinal and vertical velocities are

$$\overline{M}_u = \frac{1}{2\pi} \cos(\beta)\, c_w\, c_N \left(1 + \frac{\sin(2\zeta_m)}{2\zeta_m} \right) \quad (34)$$

and

$$\overline{M}_w = -\frac{1}{2\pi} \sin(\beta)\, c_w\, c_N \left(1 + \frac{\sin(2\zeta_m)}{2\zeta_m} \right), \quad (35)$$

where c_w denotes the chord length of the wing. The time-average of the stability derivative from the aerodynamic pitching moment, due to change in pitch rate, is zero. We can state formally that $\overline{M}_q \equiv 0$.

C. Stability Derivatives due to Change in Angle of Attack

The change in total velocity of the wing, in the wing frame, produces a change in the effective angle of attack of the wing relative to the stroke plane. For example, as detailed in [5], if the FWMAV has purely vertical velocity and increases in altitude, then the effective angle of attack and lift will be reduced. The opposite is true for a descent; the angle of attack and lift increase. The phenomenon is referred to as 'heave' damping in [5]. The change in angle of attack, $\Delta\alpha$, is either positive or negative and is obtained from:

$$\Delta\alpha = \tan^{-1}\left(\frac{v_{z,wg}}{v_{x,wg}} \right), \quad (36)$$

where $v_{x,wg}$ and $v_{z,wg}$ denote the total velocity of the wing, at the center of pressure, expressed in the wing frame in the x and z directions. In vicinity of the hover condition, we assume that the change in angle of attack is small and using the small angle assumption: $\Delta\alpha = v_{z,wg}/v_{x,wg}$. The change in angle of attack is then equal to

$$\Delta\alpha = \frac{\sin\beta\Delta u + \cos\beta\Delta w + \sin\zeta \hat{r}_2 b \Delta q}{\cos\zeta\left(\cos\beta\Delta u - \sin\beta\Delta w\right) + \hat{r}_2 b \dot{\zeta}}. \quad (37)$$

The effects of $\Delta\alpha$ will manifest in the coefficients for the normal and tangential forces, previously detailed in Eqs. (8) and (9). The resulting normal and tangential lift coefficients will be equal to

$$C_{T,\Delta\alpha} = -0.4\,\mathrm{sign}\left(\dot{\zeta}\right)\left(\cos^2(2\alpha) - 2\,\sin(4\alpha)\Delta\alpha\right) \quad (38)$$

and

$$C_{N,\Delta\alpha} = -3.4\,\mathrm{sign}\left(\dot{\zeta}\right)\left(\sin(\alpha) + \cos(\alpha)\Delta\alpha\right). \quad (39)$$

When the coefficients are substituted into the equations for lift and drag, we make the following assumption:

$$U_{cp}(t)^2 \Delta\alpha \approx \left(\mathrm{s}\beta\Delta u + \mathrm{c}\beta\Delta w + \mathrm{s}\zeta\hat{r}_2 b\Delta q\right) U_{cp}(t), \quad (40)$$

due to the fact that over the course of a flapping cycle, $U_{cp}(t) >> \Delta[.]$. The normal and tangential coefficients for the additional angle of attack are:

$$c_{T,\Delta\alpha} = 0.4\rho\, A_w \sin(4\alpha_m)\left(\hat{r}_2 b\, \omega\zeta_m\right) \quad (41)$$

and

$$c_{N,\Delta\alpha} = 1.7\rho\, A_w \cos(\alpha_m)\,(\hat{r}_2 b\,\omega\zeta_m)\ . \tag{42}$$

The stability derivative additions, due to the change in angle of attack, for the longitudinal motion of the FWMAV are:

$$\overline{X}_{u,\Delta\alpha} = -\frac{2}{\pi}\sin^2(\beta)\,(c_{T,\Delta\alpha}\mathrm{s}\alpha_m + c_{N,\Delta\alpha}\mathrm{c}\alpha_m) \tag{43}$$

and

$$\overline{X}_{w,\Delta\alpha} = -\frac{1}{\pi}\sin(2\beta)\,(c_{T,\Delta\alpha}\mathrm{s}\alpha_m + c_{N,\Delta\alpha}\mathrm{c}\alpha_m)\,. \tag{44}$$

The stability derivatives affecting the vertical motion of the FWMAV are:

$$\overline{Z}_{u,\Delta\alpha} = \frac{1}{\pi}\sin(2\beta)\,(c_{T,\Delta\alpha}\mathrm{s}\alpha_m - c_{N,\Delta\alpha}\mathrm{c}\alpha_m) \tag{45}$$

and

$$\overline{Z}_{w,\Delta\alpha} = \frac{2}{\pi}\cos^2(\beta)\,(c_{T,\Delta\alpha}\mathrm{s}\alpha_m - c_{N,\Delta\alpha}\mathrm{c}\alpha_m)\,. \tag{46}$$

The stability derivative of the aerodynamic moment, due to pitch rate, is no longer identically zero. The stability derivative, $\overline{M}_{q,\Delta\alpha}$ is calculated according to:

$$\begin{aligned}\overline{M}_{q,\Delta\alpha} \quad = \quad & -\frac{1}{\pi}\left(1 - \frac{\sin(2\zeta_m)}{2\zeta_m}\right)(\hat{r}_2 b)^2 \\ & *\Big(c_{T,\Delta\alpha}\mathrm{s}(\alpha_m) + c_{N,\Delta\alpha}\mathrm{c}\alpha_m\Big).\end{aligned} \tag{47}$$

Without the addition of the stability derivatives due to $\Delta\alpha$, the analysis does not produce the results consistent with previous studies.

V. Results

A. Variation with Stroke Plane Angle

Results are presented for a FWMAV with hawkmoth type body parameters. The flapping frequency is set at 21 Hz with an amplitude $\zeta_m = 60°$. A simple bisection algorithm, between 0° and 45°, is used to determine the angle of attack to maintain a hover condition. The bisection algorithm calculates an angle of attack of 35.895°. The stability derivatives are non-dimensionalized in the manner presented in [2], [3], and [4]. The reference length is c, the reference velocity is U, and the reference time is c/U. The reference velocity, U, is defined as:

$$U = 4\zeta_m f \hat{r}_2 b. \tag{48}$$

The non-dimensional stability derivatives, denoted by a superscript $+$, are calculated in the following manner:

$$\overline{X}_{[.]}{}^{+} = \frac{\overline{X}_{[.]}}{\rho U^2 A_w},\ \overline{Z}_{[.]}{}^{+} = \frac{\overline{Z}_{[.]}}{\rho U^2 A_w},\ \overline{M}_{[.]}{}^{+} = \frac{\overline{M}_{[.]}}{\rho U^2 A_w c}. \tag{49}$$

The stability derivatives due to the pitch rate, q, are non-dimensionalized by multiplying the denominator by an additional reference length. The mass of the system, mass moment of inertia, and gravity are non-dimensionalized according to:

$$m_{sys}{}^{+} = \frac{m_{sys}}{\rho A_w c},\ I_{yy}{}^{+} = \frac{I_{yy}}{\rho A_w c^3},\ \text{and}\ g^{+} = \frac{gc}{U^2}. \tag{50}$$

Fig. 4 shows the variation of the pole locations for a hawkmoth-sized FWMAV for changes in the stroke plane angle. To maintain the equilibrium at hover, the nominal pitch angle also changes. The stroke plane angle, β, varies from $\beta \in [0\ -22.5\ -45]$ and the corresponding nominal pitch angle is $\theta_o \in [0\ 22.5\ 45]$. Both angles are given in degrees.

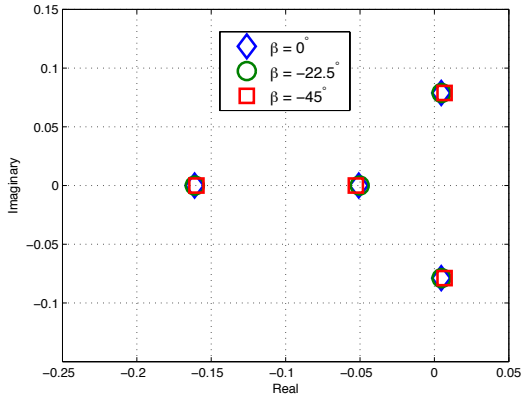

Fig. 4. Variation of Pole Locations with Stroke Plane Angle β

For a pitch angle of zero degrees, the system has two stable poles and a pair of unstable, oscillatory poles. As the pitch angle increases, the magnitude of the stroke plane angle changes to maintain the equilibrium condition. The magnitude of the poles varies slightly with the change in nominal pitch angle and stroke plane angle. The modal structure is consistent with the independent results presented in [3], [4], and [5].

The magnitude of the poles differs from the previous efforts. The unstable oscillatory mode has a slower time constant then the work in [4], but does not differ greatly from [5]. The slower of the two subsidence modes is faster than the results in [4]. The discrepancy in the magnitude of the eigenvalues could be a result of the numerous assumptions used to obtain the approximate model. In [4], the Navier-Stokes equations are coupled with the flight dynamics equations to compute the equilibrium solution at hover. The aerodynamic model is a simple quasi-steady/blade element model. The assumption on the angle of attack results in the neglect of the rotational lift effects of the wing. The wingstrokes in [4] and [5] are more complicated and biomimetic. However, the wingstroke chosen here can be replicated by current technology [18].

B. Variation of Model Insect

The modal structure for different model insects is now presented, based off of the parameters and analysis in [4]. The four model insects are a hoverfly (HF), dronefly (DF), cranefly (CF), and hawkmoth (HM). Table I details the pertinent parameters for each model. For all model insects, the nominal pitch angle is set at $\theta_o = 25°$ and the associated

Model	m (mg)	b (mm)	c (mm)	$\zeta_m(^\circ)$	f (Hz)	$\alpha_m(^\circ)$
HF	27.3	9.3	2.2	45	160	21.57
DF	68.4	11.4	3.19	54.5	157	15.49
CF	11.4	12.7	2.38	60	45.5	19.86
HM	1648	51.9	18.26	60.5	26.3	22.63

TABLE I
MODEL PARAMETER SUMMARY

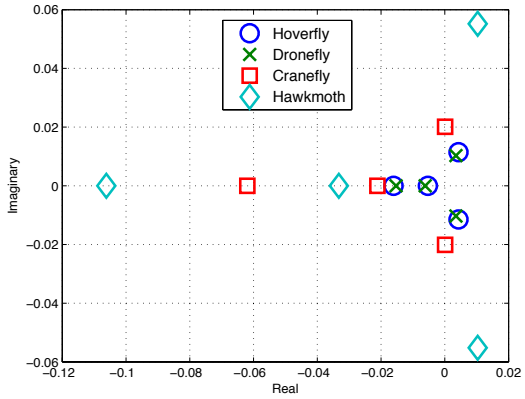

Fig. 5. Modal Structure for Multiple Insects Models

stroke plane angle is $\beta = -25^\circ$. The associated modal structure is presented in Fig. 5. The modal structure is consistent with the results presented in [4] and [5], as stated previously. As shown in [4], the stability derivatives for the dronefly and the hoverfly are nearly identical. The magnitude of the slow subsidence mode is larger than expected from the results in [4], but the magnitude of the fast subsidence mode has less than ten percent error for all species. The results in [4] predict approximately a half to full order of magnitude difference between the slow and fast subsidence mode. The worse approximation is of the unstable oscillatory mode for the cranefly; the results differs by over an order of magnitude. The sources of discrepancy are numerous and include the wingstroke assumptions, wing planform instructions, and the simplified aerodynamic model. Additional analysis will be needed to determine the effects, or lack thereof, of the individual assumptions on the results.

VI. CONCLUSION

We presented an effort to obtain an analytically tractable approximation of the stability derivatives of a flapping wing micro-air vehicle in hover. The eigenvalues are obtained using an aerodynamic model that uses perturbed velocities of the central body in the wing frame and local averaging over the course of one flapping cycle. The predicted modal structure is consistent with previous numerical and frequency domain efforts. The analysis provides a computationally efficient manner to approximate the stability of potential flapping wing micro-air vehicles in the vicinity of a hover condition. Assumptions can be changed and sizing parameters changed, to fit a potential design and analyze the potential stability.

The analysis will provide a basis for the calculation of the eigenvalues of a flapping wing MAV in other flight conditions, as well as with the inclusion of the effects of the mass of the wings on the position and orientation of the central body. Numerous simplifying assumptions are utilized to obtain an analytical results for the stability derivatives that is consistent with previous efforts. The analysis will be repeated with more complicated aerodynamic models, biomimetic wing structures, and more complicated wing kinematics, in order to gauge the sensitivity to aerodynamic inputs.

REFERENCES

[1] G. Taylor and A. Thomas, "Dynamic flight stability in the desert locus *Schistocerca gregaria*," *The Journal of Experimental Biology*, vol. 206, pp. 2803–2829, 2003.

[2] B. Etkin and L. Reid, *Dynamics of flight*. New York, NY: John Wiley and Sons, 1996.

[3] M. Sun and Y. Xiong, "Dynamic flight stability of a hovering bumblebee," *The Journal of Experimental Biology*, vol. 208, pp. 447–459, 2005.

[4] M. Sun, J. Wang, and Y. Xiong, "Dynamic flight stability of hovering insects," *Acta Mechanica Sinica*, vol. 208, pp. 447–459, 2007.

[5] I. Faruque and J. Humbert, "Dipteran insect flight dynamics. part 1 longitudinal motion about hover," *Journal of Theoretical Biology*, vol. 264, pp. 538–552, 2010.

[6] ——, "Dipteran insect flight dynamics. part 2 lateral-directional motion about hover," *Journal of Theoretical Biology*, vol. 265, pp. 306–313, 2010.

[7] J. Franklin, *Dynamics, Control, and Flying Qualities of V/STOL Aircraft*. Reston, VA: American Institute of Aeronautics and Astronautics, 2002.

[8] C. Orlowski and A. Girard, "Modeling and simulation of nonlinear dynamics of flapping wing micro air vehicles," *AIAA Journal*, vol. 49, no. 5, pp. 969–981, 2011.

[9] X. Deng, L. Schenato, W. Wu, and S. Sastry, "Flapping flight for biomimetic robot insects: Part i - system modeling," *IEEE Transactions on Robotics*, vol. 22, no. 4, August 2006.

[10] X. Deng, L. Schenato, and S. Sastry, "Flapping flight for biomimetic robot insects: Part ii - flight control design," *IEEE Transactions on Robotics*, vol. 22, no. 4, August 2006.

[11] D. Doman, M. Oppenheimer, and D. Sigthorsson, "Dynamics and control of a minimally actuated biomimetic vehicle: Part i - aerodynamic model," in *Proceedings of the AIAA Guidance, Navigation, and Control Conference, Chicago, Illinois, USA, August 10-13, 2009*. AIAA, 2009.

[12] M. Oppenheimer, D. Doman, and D. Sigthorsson, "Dynamics and control of a minimally actuated biomimetic vehicle: Part ii - control," in *Proceedings of the AIAA Guidance, Navigation, and Control Conference, Chicago, Illinois, USA, August 10-13, 2009*. AIAA, 2009.

[13] ——, "Dynamics and control of a biomimetic vehicle using biased wingbeat forcing functions: Part i - aerodynamic model," in *Proceedings of the 48th AIAA Aerospace Sciences Meeting Including the New Horizons Forum and Exposition, Orlando, Florida, USA, January 4-7, 2010*. AIAA, 2010.

[14] D. Doman and M. O. D. Sigthorsson, "Dynamics and control of a biomimetic vehicle using biased wingbeat forcing functions: Part ii - control," in *Proceedings of the 48th AIAA Aerospace Sciences Meeting Including the New Horizons Forum and Exposition, Orlando, Florida, USA, January 4-7, 2010*. AIAA, 2010.

[15] J. Sanders, F. Verhulst, and J. Murdock, *Averaging Methods in Nonlinear Dynamical Systems Second Edition*. New York, NY: Springer Science, 2007.

[16] W. Gröbner and N. Hofreiter, *Integraltafel*. Vienna, Austria: Springer-Verlag, 1949.

[17] I. Gradshteyn and I. Ryzhik, *Table of Integrals, Series, and Products Fifth Edition*. San Diego, CA: Academic Press, Limited, 1994.

[18] R. Wood, "The first takeoff of a biologically inspired at-scale robotic insect," *IEEE Transactions on Robots*, vol. 24, no. 2, pp. 341–347, 2007.